

X-ray excitation fluorescence spectra of the Eu^{2+} -stabilized V_K center in alkaline-earth fluoride mixed-crystal systems

K. Kawano, T. Ohya, T. Tsurumi, K. Katoh, and R. Nakata

Department of Electronic Engineering, The University of Electro-Communications, Chofu, Tokyo, Japan 182-8585

(Received 13 April 1998; revised manuscript received 21 December 1998)

X-ray excitation fluorescence spectra were investigated for $\text{MF}_2:\text{Eu}$ ($M = \text{Ca}, \text{Sr}, \text{and Ba}$) and their mixed-crystal systems, $\text{Ca}_{1-x}\text{Sr}_x\text{F}_2$ and $\text{Sr}_{1-x}\text{Ba}_x\text{F}_2$ with the same fluorite structure. The UV recombination fluorescence band of the V_K center associated with blue emission due to the $f-d$ transition of Eu^{2+} ions was observed with changing mixture ratios x at room temperature. Two sets of weak spectra due to $f-f$ transitions of Eu^{3+} ions also appeared in the 500–600-nm wavelength region. The peak wavelengths and the integrated intensities of the observed fluorescence were investigated as a function of the Eu concentration as well as the mixture ratio. For the blue emission of Eu^{2+} , pulsed x-ray excitation resulted in shorter lifetimes (500–800 ns) than optical excitation, suggesting energy transfers between the excited states of V_K centers and Eu^{2+} . A kinematical fluorescence mechanism was proposed, taking into account the formation of a close pair of a hopping V_K center and an immobile Eu^{2+} ion followed by an energy transfer from the former to the latter. Based on the calculated fluorescence decay curves best fitted to the response curves by x-ray pulse excitation, the energy transfer rates from V_K centers to Eu^{2+} were estimated. [S0163-1829(99)10941-X]

I. INTRODUCTION

Radiation damage studies have contributed significantly to our understanding of defect creation and interaction. Under ionizing radiation such as x rays and γ rays, the appearance of a variety of lattice defects in solid crystals have attracted the interest of many researchers in the fields of solid-state physics and scintillation materials research.^{1,2} Fluorescence studies of alkaline-earth fluorides, as both indigenous lattice ions and/or impurities, have revealed the characteristic properties of the electron-hole pairs formed.³ Extensive investigations have been carried out on trapped holes like V_K centers and trapped excitons in alkaline earth fluorides doped with Tm^{3+} ions.³⁻⁵ The trapping of an electron by a Tm^{3+} ion results in the formation of a Tm^{2+} ion with a consequent reduction in electron-hole recombination. In this process, the V_K centers can interact more stably with the nearby Tm^{2+} ions at room temperature. Meanwhile, a series of fluorescence excitation spectra such as vacuum ultraviolet excitation⁶ and core valence transition spectra^{7,8} were investigated by Russian physicists in the high-energy region of over 5 eV for fluorite-type crystals containing Ce^{3+} , Eu^{3+} , and Dy^{3+} as impurities or defect centers. Alkaline-earth fluorides offer attractive possibilities for scintillation research studies because of the advantages of the crystal stability and high luminosity of doped rare-earth ions. In particular, BaF_2 and impurity-doped BaF_2 systems⁹⁻¹¹ possess very short fluorescence lifetimes and offered potential for the development of new scintillators.

The fabrication of a mixed crystal composed of two scintillation crystals is expected to enhance the scintillation capability of the mixed crystals resulting in a higher luminosity and shorter lifetime. As the hottest example, $\text{BaFX}:\text{Eu}^{2+}$ ($X = \text{Br}, \text{I}$) phosphors obtained by replacing half the fluorine in BaF_2 with other halides have been applied as the imaging plate (IP) that is a computerized digital radiograph providing

read-write functions of photostimulated fluorescence and defect memories.^{12,13} Extensive studies on other intrinsic and doped fluorite-type crystals as well have been performed to date.³ However, there have been no reports on the control of the scintillation parameters of materials fabricated by varying the cation ratios of the systems.

In this paper, we present the studies of x-ray excitation fluorescence spectra of Eu ions doped with two series of mixed-crystal systems $\text{Ca}_{1-x}\text{Sr}_x\text{F}_2$ and $\text{Sr}_{1-x}\text{Ba}_x\text{F}_2$, at mixture ratios x in the range of 0 to 1. The experiments were performed using only *as-grown* crystals rather than *after-irradiated* ones.

Usually, the V_K center is a predominant hole center formed when alkaline-earth fluorides are x-ray irradiated at 77 K. At around room temperature, the V_K center or self-trapped hole moves through the fluorite-type lattice with a hopping motion which is qualitatively different from the behavior of electrons in the conduction band. This motion can be regarded as a succession of “random independent jumps” between equivalent sites in the lattice.^{1,3}

An Eu ion in alkaline-earth fluoride crystal prefers, uniquely, a divalent state rather than the trivalent one favored by other rare-earth ions. This suggests that an immobile Eu^{2+} ion substituted for a cation may attract a nearby V_K center in a stable manner. In this situation, the Eu^{3+} ion does not participate in the formation of the V_K center, unlike the Tm^{3+} ion.³⁻⁵ Actually, in an intermediate region of mixture ratios in a $\text{Ca}_{1-x}\text{Sr}_x\text{F}_2$ system, a temporal decrease in the emission yield of the V_K center was observed. This can be qualitatively explained by considering the formation of a close pair of V_K centers and Eu^{2+} due to the aggregation of defects surrounding an Eu^{2+} ion and subsequent energy transfers from the V_K center to Eu^{2+} . Moreover, the dependence of the intensities of UV and blue bands on the Eu concentration revealed evidence of energy transfers between the V_K center and Eu^{2+} ion because the intensity of the

former decreases with an increase in Eu concentration. The first observation of the spectra of Eu ions in the trivalent state for mixed-crystal systems is reported, although the existence of Eu^{3+} has already been revealed for the special case of $\text{CaF}_2:\text{Eu}$ grown using the fluoridizing additive method.¹⁴⁻¹⁷ From x-ray pulse excitation experiments, the lifetimes of blue fluorescence were investigated for various mixture ratios and Eu concentrations. Last, the fluorescence mechanism is discussed on the basis of the rate equations between Eu^{2+} and the V_K center, and the results of the intensity balances between the observed spectra are explained according to the proposed mechanism.

II. EXPERIMENTAL DETAILS

The single crystals used for the present investigation were grown in the authors' laboratory by the Bridgman technique.^{18,19} With the mixture molar ratio x ($0 \leq x \leq 1$), powder mixtures of CaF_2 and SrF_2 for $\text{Ca}_{1-x}\text{Sr}_x\text{F}_2$, and those of SrF_2 and BaF_2 for $\text{Sr}_{1-x}\text{Ba}_x\text{F}_2$ were arranged together with constant molar fractions of Eu^{2+} dopants of 0.05 and 0.5 mol %. The quality of CaF_2 , SrF_2 , and BaF_2 crystals was excellent, although for their highly mixed crystals, the cleavage feature along the [111] crystal axis was slightly indistinct. The results of 2θ -angle x-ray-diffraction studies, however, showed²⁰ that the lattice parameters of $\text{Sr}_{1-x}\text{Ba}_x\text{F}_2$ changed smoothly in proportion to the mixture ratio, reflecting uniform mixing throughout the entire crystal system. ESR (electron spin resonance) studies²⁰ for a Eu^{2+} ion doped into the same mixed-crystal system revealed evidence of distortion compensation for lattice misfit at local sites in the mixed crystal by the addition of low-symmetry crystal fields. Infrared and Raman measurements³ on $\text{Ca}_{1-x}\text{Sr}_x\text{F}_2$ and $\text{Ba}_{1-x}\text{Sr}_x\text{F}_2$ systems were reported by Verleur and Barker²¹ and Lacina and Pershan,²² and theoretical models with possible configurations of a fluorine ion and its nearest-neighbor cations were proposed.

The x rays for excitation are generated from the x-ray source of a microfocuser analyser (Rigaku Denki Co., Microflex-4180, 50 kV) using the $K\alpha$ line of a Cu target, with a filament current of 0.5–1 mA. A monochromator (Jobin-Yvon, H-20) with automatic wavelength scanning was used to analyze the fluorescence or scintillation light. Photomultipliers (Hamamatsu Photo. Co., R928, partly R818, 1P28) were cooled to suppress the dark current using a photomultiplier cooler (Hamamatsu Photo. Co., C659S). Optical alignment for the measurement system was performed by optimizing the output voltage of the green-blue fluorescence of a well-known scintillation crystal BGO ($\text{Bi}_4\text{Ge}_3\text{O}_{12}$).^{23,24} All fluorescence measurements (without polarization investigations) were carried out at room temperature except for some test experiments conducted at liquid-nitrogen temperature. No visible coloration of crystals was observed during the measurements.

For the precise measurement of lifetime, a continuous x-ray beam was pulsed with a much narrower pulse duration than that of the lifetime observed, and some pulse processing techniques were applied.²⁵ For deflecting the x-ray beam, a magnetic induction coil was inserted into the path of the electron beam of the x-ray microfocuser analyser.²⁶ When the direct current of the coil was switched off by a short duration

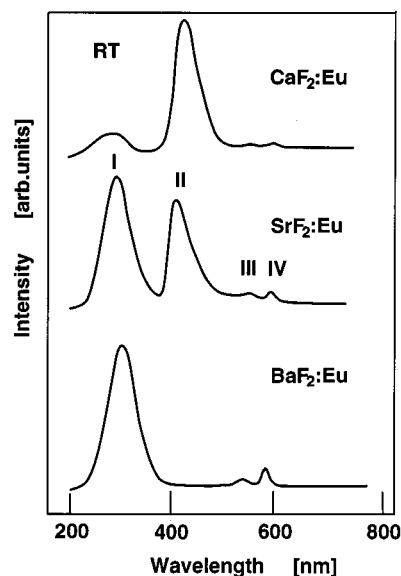


FIG. 1. Fluorescence spectra obtained by x-ray excitation for CaF_2 , SrF_2 , and BaF_2 with Eu (0.1 mol %) as dopants at room temperature. Wavelength resolution is 1 nm.

pulse triggered from a high-speed pulse driver, the electron beam could generate x-ray pulses (with a duration of 20 ns) from the Cu target. The very weak pulse signal detected was amplified using a high-speed and high-input impedance operational amplifier (NEC, μPC1664) and was accumulated using a boxcar averager (Stanford Res. Inc., SR-250 USA). The enhanced fluorescence line shape was numerically smoothed using a personal computer (NEC PC9801 Japan).

III. EXPERIMENTAL RESULTS

The x-ray excitation fluorescence spectra of doped Eu^{2+} ions are shown in Fig. 1 for three typical alkaline-earth fluoride crystals in the wavelength region of 200–800 nm at room temperature. Four bands, a UV fluorescence band (289-nm peak for $\text{SrF}_2:\text{Eu}$, indicated as band I), a blue band (411 nm indicated as band II) and two weak bands (550 nm indicated as band III and 585 nm indicated as band IV, respectively) are observed, although band II disappears for BaF_2 . As band I is observed for nondoped crystals also, it is identified as the recombination fluorescence of the V_K center, i.e., the F_2^- molecule self-trapped with a hole that is usually formed in host alkaline-earth fluoride crystals.³ This V_K center spectrum was confirmed to be more prominent in intensity at 95 K than at room temperature. Band II is the emission due to the transition of the doped Eu^{2+} ion from $4f^65d$ (e_g) to $4f^7$ (8S) because the peak energy agreed well with the result from optical excitation.^{19,27} For $\text{BaF}_2:\text{Eu}$ below liquid-nitrogen temperature, however, a broad yellow band with a 580-nm peak appears under UV light excitation whose emission has been reasonably assigned to an impurity-trapped exciton band.²⁷⁻²⁹ For CaF_2 , the integrated intensity of band I is weaker than that of band II, but for SrF_2 , the former is stronger than the latter. Bands III and IV have a common tendency of a slight increase in intensity on the order of CaF_2 , SrF_2 , and BaF_2 , in comparison with bands I and II.

The variations of the peak energy/wavelength of these

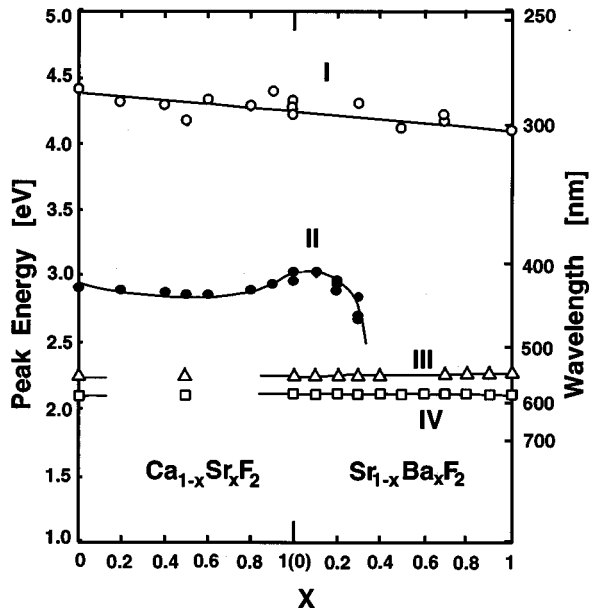


FIG. 2. The variations of the peak energy/wavelength of the UV fluorescence band (termed as band I), the blue band (band II), and the two weak bands (bands III and IV) as a function of the mixture ratio x of the two mixed-crystal systems.

four bands are shown in Fig. 2 as functions of the mixture ratio x of the two mixed-crystal systems $\text{Ca}_{1-x}\text{Sr}_x\text{F}_2$ and $\text{Sr}_{1-x}\text{Ba}_x\text{F}_2$. Band I shifts with a linear decrease in peak energy from CaF_2 to BaF_2 . The peak position and linewidth of band II coincides well with those of the strong, broad luminescence observed as the $f-d$ transition of Eu^{2+} by the excitation of THG (third harmonic wave; 354 nm) of the pulsed yttrium aluminum garnet (YAG) laser.^{18,19,27} Consistency with the optical results is also confirmed by the characteristic behavior wherein the peak wavelength of band II moves to a longer wavelength for intermediately mixed crystals between CaF_2 and SrF_2 . For the band II peak, the longest wavelength emission reaches 434 nm for a half mixed $\text{Ca}_{0.5}\text{Sr}_{0.5}\text{F}_2:\text{Eu}$ crystal. This nonlinear behavior in peak energies has previously been explained as a contribution of the electron-phonon interaction rather than the inhomogeneous effect due to formation of mixed crystals.^{18,19} For the $\text{Sr}_{1-x}\text{Ba}_x\text{F}_2$ system, on the other hand, band II moves once to a longer wavelength similar to the $\text{Ca}_{1-x}\text{Sr}_x\text{F}_2$ system, but disappears abruptly as it approaches BaF_2 . This phenomenon is explained by the excited states of Eu^{2+} degenerating with the conduction band in Ba-rich crystals, and a new yellow emission of impurity-trapped exciton replacing the blue emission at low temperatures.²⁷⁻²⁹ Bands III and IV with peak wavelengths independent of the mixture ratio arise due to the transitions of a small amount of Eu^{3+} which are usually assigned to the two transitions from $^5\text{D}_0$ to $^7\text{F}_1$ and $^5\text{D}_0$ to $^7\text{F}_2$, respectively, as observed in several Eu^{3+} -salts.³

Figure 3 shows the variations of the integrated fluorescence intensities of the observed bands as a function of the mixture ratio x for the two mixed-crystal systems with 0.05 mol % Eu. It is noted that the intensity of band I becomes weak in the intermediate mixture regions for both the mixed-crystal systems. For band II in the $\text{Ca}_{1-x}\text{Sr}_x\text{F}_2$ system, however, the intensity increases slightly once, around $x=0.2$ be-

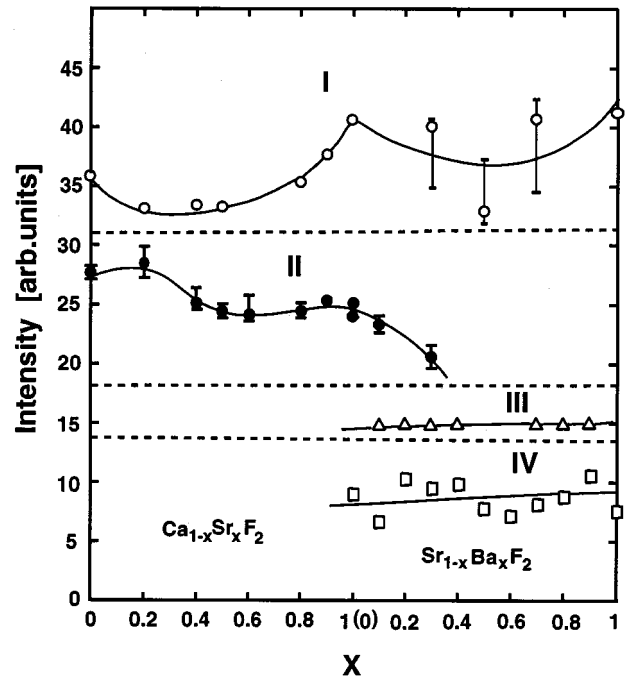


FIG. 3. Variations of the integrated fluorescence intensities of the observed bands as a function of the mixture ratio x . Magnitude of the respective intensity indicates the relative change in each band but not interbands.

fore decreasing to the minimum around $x=0.5$. This temporal anomalous increase in the intensity was confirmed not only in a similar experiment using another sample series with the same Eu concentration, but also from the results obtained using pulsed x rays as described later. The mixture ratio dependence of the relative intensity ratio $S_{\text{II}}/S_{\text{I}}$ of band II to band I is shown in Fig. 4. We can see that the ratio shows an anomalous hump and the value of the $S_{\text{II}}/S_{\text{I}}$ ratio becomes 5 around $x=0.2$, at which the emission of Eu^{2+} ions is enhanced, compensating for the decrease in the emission of the V_K center. Bands III and IV for the $\text{Sr}_{1-x}\text{Ba}_x\text{F}_2$ system commonly exhibited a slight increase in their intensities in all regions with increasing x value. From the observed intensity ratios of bands III and IV to band II except for the Ba-rich $\text{Sr}_{1-x}\text{Ba}_x\text{F}_2$ system, the population fraction of

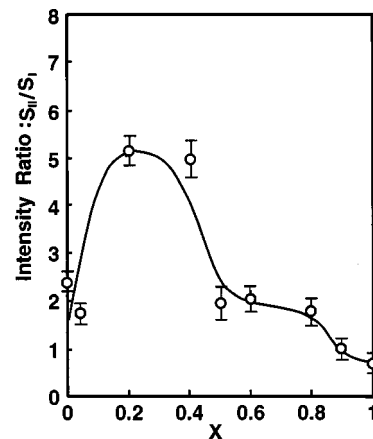


FIG. 4. Mixture ratio x dependence of relative intensity ratio $S_{\text{II}}/S_{\text{I}}$ of band II to band I.

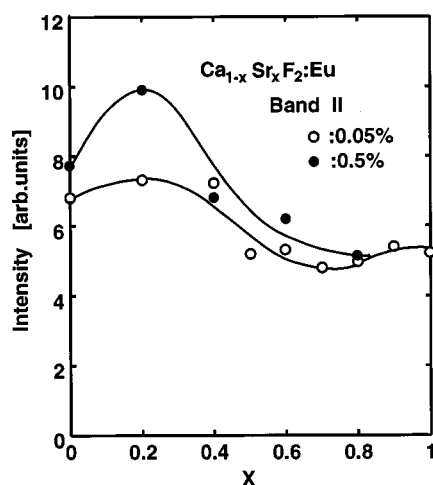


FIG. 5. Mixture ratio x dependences of pulse fluorescence intensities of band II under x-ray pulse (duration: 20 ns) excitation with 0.05 and 0.5 mol % Eu concentrations in the $\text{Ca}_{1-x}\text{Sr}_x\text{F}_2$ system.

Eu^{3+} of all the doped Eu concentrations was estimated to be on the order of one-hundredth. This is in good accordance with the result estimated from the optical excitation^{19,27} and ionic thermocurrent (ITC) experiments carried out by our group.³⁰ It implies that the probability of ionization from Eu^{2+} to Eu^{3+} during the experiments of x-ray excitation is very small in the present systems. For the Ba-rich $\text{Sr}_{1-x}\text{Ba}_x\text{F}_2$ system, bands III and IV retain their intensities even after the disappearance of band II. This indicates that the emissions of bands III and IV are predominantly caused by reabsorption of the fluorescence of band I because the optical excitation spectra of these bands in the 500–600 nm wavelength region are observed as sharp lines at the 390 nm, 375 nm, and other fine spectra around 300 nm corresponding to the f - f transition absorptions of Eu^{3+} ($4f^6$) ions.³¹

The x -dependence of the fluorescence intensity of band II under x-ray pulse excitation is shown in Fig. 5 for 0.05 and 0.5 mol % of Eu in the $\text{Ca}_{1-x}\text{Sr}_x\text{F}_2$ system. It is again emphasized here that the intensity of band II is maximal around $x=0.2$, independent of the Eu concentration. The intensity maximum is highly enhanced in the case of higher Eu concentration. This evidence is consistent with the result that the peak position for the response function under x-ray pulse excitation exhibits an anomalous decrease near $x=0.2$ which is explained in a later section (Fig. 9). The variation of the integrated fluorescence intensities of bands I and II against the Eu concentration in $\text{CaF}_2:\text{Eu}$ is shown in Fig. 6. It is observed that the intensity of band I decreases with the Eu concentration, whereas band II has the maximal fluorescence intensity for the Eu concentration of 0.2 mol %. This suggests that the increase of Eu concentration up to 0.2 mol % enhances energy transfers from V_K centers to Eu^{2+} because the concentration of the V_K center formed is thought to be constant independent of the Eu concentration. The slight decrease in intensity of band II for 0.5 mol % Eu corresponds likely to the phenomenon of concentration quenching among Eu^{2+} ions with higher densities. In the optical excitation results, on the other hand, the intensity of band II exhibited a maximum at 0.05 mol % Eu concentration.¹⁹ The variation of the lifetime of band II with respect to the mixture ratio for

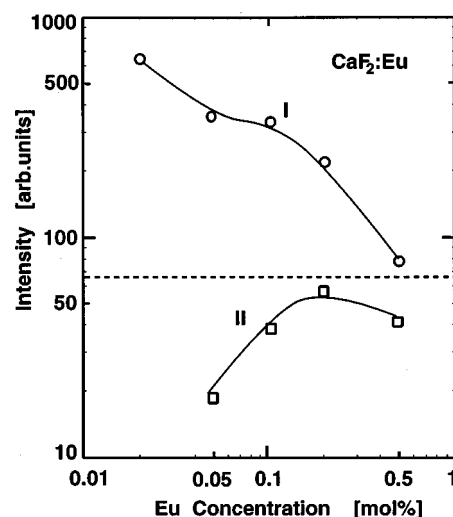


FIG. 6. Variations of the fluorescence intensities of band I and band II as a function of the Eu concentration for $\text{CaF}_2:\text{Eu}$.

0.05 and 0.5% Eu concentrations in $\text{Ca}_{1-x}\text{Sr}_x\text{F}_2$ mixed-crystal systems is shown in Fig. 7. For all the values of x , the higher concentration (0.5 mol % of Eu) crystals have shorter lifetimes than the lower concentration (0.05 mol % of Eu) ones. The lifetime decreases monotonically with increasing x ; from 830–520 ns and from 640–470 ns for the 0.05 and 0.5 mol % crystals, respectively. A similar result was obtained in our earlier investigation¹⁹ performed using the optical excitation of UV light, in which the decrease in the lifetime was due to the increase in nonradiative rates caused by the decrease of thermal activation energy with increasing x . The lifetime for $\text{CaF}_2:\text{Eu}$ becomes short with increasing Eu concentration, as shown in Fig. 8. We note here¹⁹ that the results of UV laser excitation had revealed a lifetime of 1 μs or more for the same blue band of the corresponding concentrations of Eu. The shorter lifetimes obtained with x-ray excitation mean that the blue fluorescence of Eu^{2+} does not originate from the reabsorption of the fluorescence of V_K centers, in which the optical absorption bands have their peaks at 214 and 334 nm for $\text{CaF}_2:\text{Eu}$,^{18,19} but is emitted via

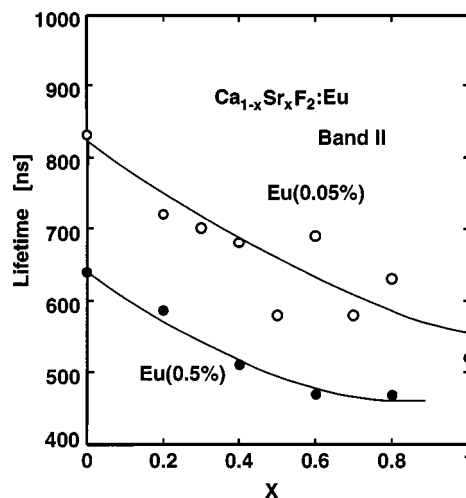


FIG. 7. Variations of the lifetimes of band II at 0.05 and 0.5% Eu concentrations as a function of x in $\text{Ca}_{1-x}\text{Sr}_x\text{F}_2$ mixed-crystal systems.

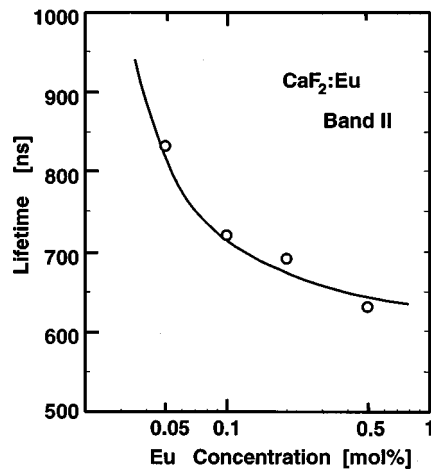


FIG. 8. Variation of the lifetime of band II as a function of the Eu concentration for $\text{CaF}_2:\text{Eu}$ crystals.

energy transfers from the excited state $^1\Sigma_u$ of V_K centers to the excited state e_g of Eu^{2+} . The results of extremely short lifetimes of V_K centers (CaF_2 ; 49 ns, SrF_2 ; 19 ns, BaF_2 ; 7.7 ns) obtained by Ershov, Zakharov, and Rodnyi⁷ support this consideration.

The fluorescence decay feature of band II for a pulse x-ray excitation was analyzed, particularly taking consideration of the variation of the time t_{\max} that gives a peak value, in the fluorescence decay curve. The x dependence of t_{\max} is shown in Fig. 9 for 0.05 and 0.5 mol % of Eu in $\text{Ca}_{1-x}\text{Sr}_x\text{F}_2$ mixed-crystal systems with the inset indicating the position of t_{\max} in a typical line shape. The t_{\max} is minimal around $x=0.2$ regardless of Eu concentration, in which the half-width of the decay curve becomes much narrower.

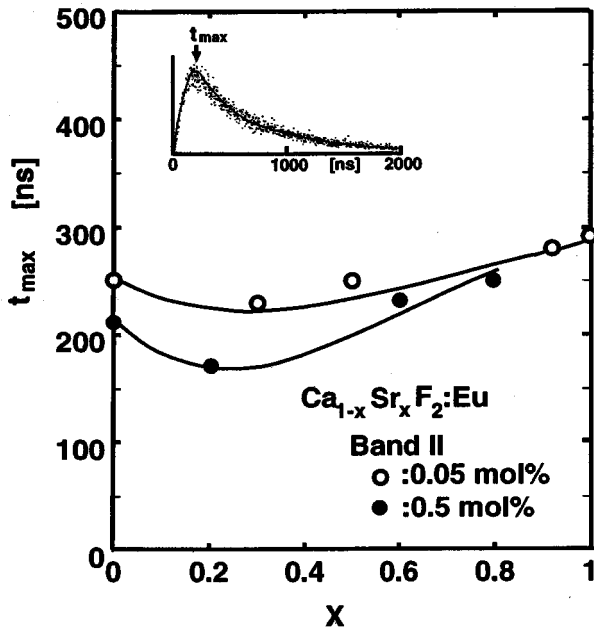


FIG. 9. Mixture ratio x dependence of the peak time t_{\max} in the fluorescence decay curve of band II. The position of t_{\max} in the decay line shape is shown in the inset indicating the raw experimental data and the best-fit curve at $x=0.2$.

IV. DISCUSSION

A. Hopping migration of the V_K center and its close pair formation with the Eu^{2+} ion

In earlier studies of x-ray excitation for alkaline-earth fluoride crystals,^{3,4} it was reported that doped Tm^{3+} ions induced two main kinds of fluorescence besides temperature-dependent defects, one from the V_K center which was a hole-trap molecule consisting of a pair of fluorine ions and the other from the $f-f$ transitions of Tm^{3+} , to which the normal emission by UV-light excitation corresponded. They also determined that although the V_K centers might be produced by nondoped CaF_2 crystals at 77 K, their initial rate of production could be increased by more than one order of magnitude if the crystals were doped with trivalent rare-earth ions like Tm^{3+} .⁵ The temperature dependence results suggested that the V_K centers were formed preferentially near Tm^{2+} sites retrapping some of the moving holes to form impurity-stabilized hole centers. In the present study, however, the Eu ion in alkaline-earth fluoride crystal prefers uniquely a divalent rather than trivalent state, different from the other rare-earth ions, which suggests that Eu^{2+} ions may attract nearby V_K centers in a more stable manner than Tm^{3+} ions.

When we consider the radiation effect from a universal point of view for the present mixed-crystal systems, we propose that the generated number of V_K defect centers increases from CaF_2 to SrF_2 to BaF_2 due to the following two reasons. First, during the fabrication of mixed crystals, the valence bands commonly constitute $2p$ orbitals in F^- ions while the conduction bands consist of $4s$ orbitals for Ca^{2+} , $5s$ ones for Sr^{2+} , and $6s$ ones for Ba^{2+} , respectively. The decrease in the energy band gaps from CaF_2 (12.2 eV) to SrF_2 (11.44 eV) to BaF_2 (10.59 eV) (Ref. 3) will result in the transfer of conduction electrons from the Ca and the Sr sites to the Ba site. As band I is emitted by electron trappings of V_K centers, this mixture process will lead to an increase in the fluorescence intensity of V_K centers in the sequence of CaF_2 , SrF_2 , and BaF_2 . Second, there exists a condition that the probability of photoelectric absorbance of host crystals of x-ray radiation increases in proportion to the fifth power of the atomic number of irradiated crystals.³¹ These two factors result in the formation of a large number of V_K defects in the above succession of crystals. We found, however, as shown in Fig. 3, that the intensity of the V_K band decreased temporarily in the intermediate region of mixed ratios, particularly in the $\text{Ca}_{1-x}\text{Sr}_x\text{F}_2$ system, although the number of V_K centers themselves should actually increase. Therefore we consider that this anomalous decrease is caused by energy transfers from V_K centers to Eu^{2+} because the distance between them decreases down due to interdefect interaction. The incorporation of impurity ion into host alkaline-earth fluoride crystal forces the shift from the normal positions of the surrounding F^- ions due to the differences in ionic radii between the alkaline-earth cation and the impurity ion substituted for it. This effect is further enhanced by the formation of mixed crystals. The atomic displacements of F^- ions create small distortion points in the lattice and form F_2^- molecules or V_K centers during x irradiation. Since substituted Eu^{2+} ions and alkaline-earth cations are isovalent to host cations, they do not form any electric dipoles, and are immobile in the lattices. It should be noted that the Eu^{3+} ion was

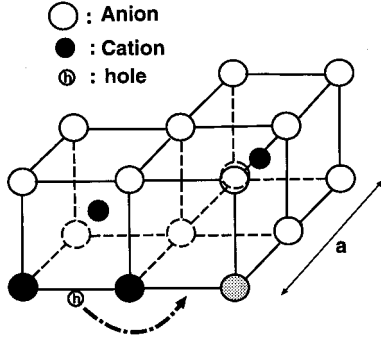


FIG. 10. Schematic diagram of the 180° jump available to the V_K center (F_2^- +hole) in the alkaline-earth fluoride lattice with the lattice parameter a .

not involved in this process because there was no proof of hole migration from Eu^{3+} to Eu^{2+} ions in the experiment. On the other hand, V_K centers are in polarized states and approach each other by dipole-dipole interactions. Such aggregation phenomena would result in the gathering of V_K centers around an immobile Eu^{2+} ion as a defect center.³² The fabrication of mixed crystals would induce more distortion points than those produced by Eu^{2+} impurities. Hence the mixed crystal with the highest mixture ratio of $x=0.5$ may have the maximum number of V_K centers. Additive distortions, however, due to the displacement of Eu^{2+} , can significantly affect the generation of V_K centers because the cation displacement polarizability becomes twice that of the anion due to the valence difference.³ The differences in the cation-anion distances between the host lattice and the substitutional Eu^{2+} -anion lattice are +3% for CaF_2 (0.2366 nm), no misfit for SrF_2 (0.2511 nm), and -3% for BaF_2 (0.2685 nm).³ Accordingly, Ca-rich crystals around $x=0.2$ in the $Ca_{1-x}Sr_xF_2$ system can produce more V_K centers surrounding the Eu^{2+} ion.

The thermally induced motion of V_K centers was studied in greater detail by Beaumont *et al.*⁴ by preferentially aligning the centers at 77 K using polarized bleaching light with $E \parallel [001]$. Based on their ESR studies, it was found that the centers which preferentially aligned along $[010]$ and $[001]$ disappeared at the same rate to complete destruction at about 138 K; it was concluded that only linear (180°) motion of V_K centers occurred in CaF_2 below the temperature of disappearance. The schematic diagram of the 180° jump available to V_K center in the alkaline-earth fluoride lattice is shown in Fig. 10. The defect may differ in size or shape from the perfect lattice it replaces. The surrounding lattice then deforms to accommodate the mechanical misfit. Moreover, the defect may introduce a modified charge distribution. Electric fields originating from the charge misfit then distort the nearby electronic and ionic distributions. This coupling between electrical and mechanical relaxation near point defects was examined precisely by Flynn³³ for continuum descriptions of the dielectric and elastic behavior to simulate the lattice surrounding defects of atomic dimensions. A cubic polar lattice (the static dielectric constant ϵ) of ions with charge $\pm Z_0e$ contributes to the polarization $\mathbf{P}(\mathbf{r})$ at the position \mathbf{r} surrounding a localized charge $\pm Ze$,

$$\mathbf{P}(\mathbf{r}) = \frac{Z|e|}{4\pi} \left(1 - \frac{1}{\epsilon} \right) \frac{\mathbf{r}}{r^3}. \quad (4.1)$$

This can be divided among the ions to yield the actual displacements. Then, the ionic displacements ξ_{\pm} in the continuum approximation are

$$\xi_{\pm} = \pm \frac{\Omega Ze}{4\pi Z_0 e^*} \left(1 - \frac{n^2}{\epsilon} \right) \frac{\mathbf{r}}{r^3}, \quad (4.2)$$

where e^* is the effective charge describing lattice polarization and Ω is the atomic volume. Using the well defined theory on polarization in ionic lattices,³³ the activation energy E_a calculated for the hopping migration of the V_K center is

$$E_a = \frac{2\pi e^2 (n^2 + 2)^2 Z^2}{27n^2 a Z_0^2} \cdot \frac{d^2}{a^2} \left(1 - \frac{n^2}{\epsilon} \right), \quad (4.3)$$

under the assumption of $q_m d \sim 0$, where q_m is the magnitude of the typical wave vector at the zone boundary, d is the jump distance, and a is the lattice parameter. For CaF_2 to SrF_2 using the typical values of $Z=Z_0/2$ (F^- ion has an effective half charge of cation³), $\epsilon=6.8-6.5$, $n=1.45-1.47$ around $\lambda=300$ nm, $a=0.545-0.578$ nm, and $a=2d$ for 180° jumps, we obtain $E_a=0.22-0.20$ eV, which is comparable with the observed activation energy of 0.31–0.30 eV.⁴ This suggests that the hopping migrations of V_K centers in the alkaline-earth fluoride lattice may result in their clustering according to their elastic and electrostatic misfits which are further enhanced by the formation of mixed crystals.

B. Energy transfers between V_K and Eu^{2+} centers

Besides V_K centers and Eu^{2+} , the ionizing yields of x ray to defect centers contribute very little to the production of intrinsic point defects in nondoped alkaline-earth fluorides.³ Also for the present mixed-crystal systems doped with Eu ions, no defect bands such as F centers, hole-trapped V_H , V_{KA} , and $V_{KA'}$ centers were observed in the measurements performed at room temperature. Since the intensities of the pair of bands III and IV were independent of the variations of V_K centers and Eu^{2+} in all the mixed-crystal systems, the ionization process from Eu^{2+} to Eu^{3+} through V_K is presumed to be unlikely during x-ray excitation measurements. Thus a model of fluorescence mechanism proposed by considering energy transfers among the observed fluorescence bands is described with greater clarity using Fig. 11. In the figure, it is indicated that the conduction electrons migrate to lower energies from Ca ($4s$) to Sr ($5s$) and enter into the degenerate states of e_g of the Ba ($6s$) conduction band. The four kinds of fluorescence observed are indicated by thick black arrows, except for the yellow emission observed below 77 K for $BaF_2:Eu$ (Ref. 27) which is attributed to be from an exciton level (e). The population migrations of electrons/holes among the energy levels of the V_K center (${}^1\Sigma_u$), Eu^{2+} ions (e_g band), and Eu^{3+} ions (5D_0) are indicated by shaded arrows.

A quantitative treatment of energy transfer between the V_K center and Eu^{2+} ion can be carried out by solving the rate equations of the population level of each center.^{34,35} The

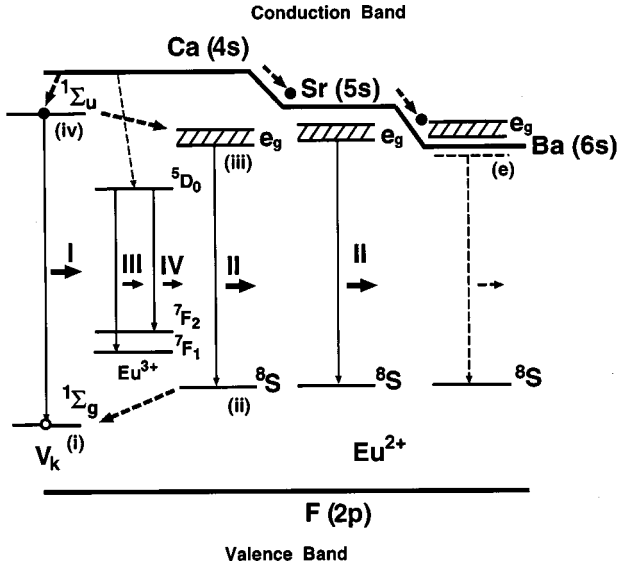


FIG. 11. A model of the fluorescence mechanism proposed by considering energy transfers among the observed fluorescence bands. Four fluorescence bands were observed: band I to IV, represented by thick-rightward arrows and thin-downward arrows showing their transitions between energy levels. For $BaF_2:Eu$, the yellow emission from an exciton level (e) observed below 77 K by optical excitation is shown by a dotted arrow. The energy transfers between the V_K center and Eu^{2+} ions are indicated by dot-shaded arrows together with the electron transfers out of the conduction band. The numbers (i)–(iv) indicate the typical levels of the four-level approximate calculation. For details, see text.

model calculation explains the anomaly that the intensity of band II shows a nonlinear decrease in Fig. 3 while the lifetime gives a monotonic decrease with increasing x in Fig. 7. In particular, the analysis of the response decay curve of fluorescence by x-ray pulse excitation is important for complete comprehension.

When x-ray energy is absorbed in a crystal, it appears in the form of electrons in an empty conduction band and holes in an occupied valence band, or in the form of excitons at lattice ions. The generated holes are trapped by distorted F_2^- molecules to emit the fluorescence of band I as a result of recombination with the electrons from the excited state $1\Sigma_u$ of the V_K center. For simplicity, the $1\Sigma_u$ state is assumed as a source level of electrons to the excited e_g level and the ground $8S$ level of Eu^{2+} , in which the population of electrons thermally migrating from the conduction band to $1\Sigma_u$ is regarded as constant. Moreover, it is assumed that electron population migrating through the paths from $1\Sigma_u$ and e_g to $5D_0$ are too small to be taken into account. These assumptions are valid because, as seen in Fig. 3, the fluorescence intensities of bands III and IV are extremely weak and independent of the mixture ratio. The generation of V_K centers and electron-hole pairs by x-ray excitation results in dynamical energy transfers depending on the distance between Eu^{2+} and the V_K center because the latter migrates by “jumping”,³ at room temperature. The V_K centers jump to nearby distortion-rich areas to occupy definite sites predominantly in high mixture ratio crystals. In order to interpret the experimental results of variations of intensities and pulse decay curves of the observed spectra, we will consider only the retaining energy transfers between V_K centers and Eu^{2+} cen-

ters. In addition, energy transfers due to Eu^{2+} - Eu^{2+} exchange interactions are ignored for the present diluted systems. Under these assumptions, we can treat the problem as a four-level system that consists of the ground $1\Sigma_g$ [described as level (i)], the excited $1\Sigma_u$ [level (iv)] in the V_K center, the e_g bottom-most level [level (iii)], and the ground $8S$ state [level (ii)] in the Eu^{2+} center. The transition probability per unit time from level i to j is expressed by p_{ij} . Both the radiationless processes, from $1\Sigma_u$ to e_g and from $8S$ to $1\Sigma_g$ are usually assumed to decay in a time of less than one nanosecond.

If N_0 denotes the total number of defects in the system and $N_1(t)$, $N_2(t)$, $N_3(t)$, $N_4(t)$ the time-variable numbers of V_K centers in the $1\Sigma_g$ state, Eu^{2+} ions in the $8S$ ground state, Eu^{2+} ions in the e_g bottom-most state, and V_K centers in the $1\Sigma_u$ state, respectively, then the rate equations among the population levels under pulse excitation are given by

$$\frac{dN_4}{dt} = -p_4 N_4 + h(t)(N_1 - N_4), \quad (4.4a)$$

$$\frac{dN_3}{dt} = -p_3 N_3 + p_{43} N_4, \quad (4.4b)$$

$$\frac{dN_2}{dt} = -p_{21} N_2 + p_{12} N_1 + p_{32} N_3 + p_{42} N_4, \quad (4.4c)$$

$$N_1 + N_2 + N_3 + N_4 = N_0, \quad (4.4d)$$

where $p_4 = p_{41} + p_{42} + p_{43}$ and $p_3 = p_{31} + p_{32}$ with $N_2(0) = N_3(0) = N_4(0) = 0$. Here, $h(t)$ may be considered to be a pulse with height h and duration ω , then,

$$h(t) = h[u(t) - u(t - \omega)], \quad (4.5)$$

where $u(t)$ is the unit step function. For $t \leq \omega$, the solutions of the above equations are obtained analytically by considering the response to a step-function pumping pulse. Using these solutions at $N_0 = 10^{19}$ and $h = 1.0$ assuming $N_2(\omega) \cong 0$, the values of two important constants $N_3(\omega)$ and $N_4(\omega)$ at $t = \omega$ are roughly determined. The solutions of $N_4(t)$ and $N_3(t)$ for $t > \omega$ are derived from the much simplified equations of Eqs. (4.4a)–(4.4d), as follows:

$$N_4(t) = N_4(\omega) \exp\{-p_4(t - \omega)\}, \quad (4.6a)$$

$$N_3(t) = \left[N_3(\omega) + \frac{p_{43} N_4(\omega)}{p_4 - p_{32}} \right] \exp\{-p_{32}(t - \omega)\} - \frac{p_{43} N_4(\omega)}{p_4 - p_{32}} \exp\{-p_4(t - \omega)\}. \quad (4.6b)$$

The decay signals of the fluorescence of band I (V_K) and band II (Eu^{2+}) follow $N_4(t)$ and $N_3(t)$ curves, respectively, in which the latter consists of two exponentials, as shown in Eq. (4.6b). If the exciting pulse is short enough, a maximum can occur for $N_3(t)$ at a time t_{\max} given by

$$t_{\max} = \frac{1}{p_4 - p_{32}} \ln \left[\frac{p_{32}}{p_4} + \frac{(p_4 - p_{32}) p_{32}}{p_4 p_{43}} \frac{N_3(\omega)}{N_4(\omega)} \right], \quad (4.7)$$

TABLE I. Comparison between the experimental and calculated values of the lifetime τ_E , the peak time t_{\max} , and the ratio of integrated intensities of S_{II} (band II; Eu^{2+} ion) to S_I (band I; V_K center) of the fluorescence decay curve for the $\text{Ca}_{1-x}\text{Sr}_x\text{F}_2:\text{Eu}$ (0.5 mol %) system under pulse x-ray excitation (duration; ω). The population ratio $N_3(\omega)/N_4(\omega)$ at $t=\omega$ and the transfer rate p_{43}/p_4 obtained from the calculation are also given.

x	τ_E (ns) [Expt.]	t_{\max} (ns) [Expt.]	t_{\max} (ns) [Calc.]	S_{II}/S_I [Expt.] [Expt.]	S_{II}/S_I [Calc.]	$N_3(\omega)/N_4(\omega)$ [Calc.]	p_{43}/p_4 [Calc.]
0	640	210	211	2.3	2.70	0.176	0.540
0.2	580	170	170	5.1	4.10	0.205	0.644
0.4	510	180	179	3.8	3.35	0.111	0.489
0.6	470	230	230	2.1	1.00	0.042	0.261
0.8	460	250	250	1.9	0.20	0.014	0.173
1.0	450	280	281	0.8	0.24	0.011	0.109

where the condition for t_{\max} to be positive must be satisfied as

$$p_4 > p_{32} \quad \text{and} \quad \frac{p_{43}}{p_{32}} > \frac{N_3(\omega)}{N_4(\omega)}. \quad (4.8)$$

Equation (4.8) represents the relation between the probability and the population when the fluorescence decays with a curve as shown in the inset in Fig. 9. We may obtain a best-fit experimental curve for band II in response to x-ray pulse ($\omega=20$ ns) excitation to Eq. (4.6b) using the numerical iteration method starting with appropriate values of p_{ij} , $N_3(\omega)$, and $N_4(\omega)$ under the conditions of Eq. (4.8). The p_{32} and p_{41} values are obtained from the experiment as reciprocals of the lifetimes τ_E for Eu emission and τ_V for V_K emission, respectively, in which τ_V values for the mixed crystals were estimated by distributing proportional to the mixture ratios using the τ_V values of CaF_2 and SrF_2 , reported by Ershov *et al.*⁷ A comparison of the experimental and calculated results is given in Table I. Besides, as the decay curve of band I is calculated from Eq. (4.6a), the ratio of the integrated intensity S_{II} (Eu^{2+} ion or band II) to S_I (V_K center or band I) for each decay curve was estimated and compared with the experimental result shown in Fig. 4. The comparison is made using the result obtained for the 0.5 mol % of Eu in the $\text{Ca}_{1-x}\text{Sr}_x\text{F}_2$ system. As seen in Figs. 3 and 5, the fluorescence intensity of band II exhibits an anomalous increase around $x=0.2$ when the intensity of band I is minimal. This evidence is qualitatively explained from the calculated results. Namely, at the mixture ratio $x=0.2$, the distribution ratio p_{43}/p_4 of transition probability becomes 0.644 indicating the highest energy transfer rate from the V_K center to Eu^{2+} when the ratio of populations $N_3(\omega)$ and $N_4(\omega)$ becomes 20% at $t=\omega$. The variation of this ratio for x traces generally the experimental result of the dependence of the S_{II}/S_I ratio.

The results of Tm^{3+} in alkaline-earth fluoride crystals^{3,4} have shown that V_K centers accompanied by ionic displace-

ments were liable to be located close to the hole-released Tm^{2+} ions. The situation is also predicted in the case of Eu^{2+} doped into the present $\text{Ca}_{1-x}\text{Sr}_x\text{F}_2$ mixed-crystal system, although Eu^{3+} is not concerned. Substitution of the cations between Ca^{2+} and Sr^{2+} in the mixture system would produce even more distortions of crystal lattices because of the large differences in their ionic radii. Meanwhile, there exists the peculiarity that the ionic radii of Eu^{2+} and Sr^{2+} are so close that the distortions will be enhanced in Ca-rich crystals for $x<0.5$, as obtained by the present experiment, in which the quantum efficiency of the fluorescence of Eu^{2+} increases.

V. CONCLUSIONS

X-ray excitation fluorescence spectral studies were carried out on Eu ion-doped fluorite-type $\text{Ca}_{1-x}\text{Sr}_x\text{F}_2$ and $\text{Sr}_{1-x}\text{Ba}_x\text{F}_2$ mixed-crystal systems. The following conclusions were drawn from the present investigation.

(i) The four sets of bands observed were explained, and the relationship between their integrated intensities and the mixture ratios was given for the $\text{Ca}_{1-x}\text{Sr}_x\text{F}_2:\text{Eu}$ system.

(ii) The V_K centers were formed in a stable manner by the incorporation of Eu^{2+} ions rather than Eu^{3+} ions.

(iii) The blue fluorescence of Eu^{2+} did not originate from the reabsorption of the V_K fluorescence but was emitted via energy transfers from the excited state $^1\Sigma_u$ of V_K to the e_g band of Eu^{2+} .

(iv) A model of the four-level fluorescence mechanism, taking into consideration the lattice distortions due to the formation of mixed crystals and the hopping of the V_K center followed by energy transfers to the Eu^{2+} center, was proposed.

ACKNOWLEDGMENTS

The present work was supported by a Grant-in-Aid for Scientific Research on Priority Areas ‘‘New Development of Rare Earth Complexes’’ No. 06241227 and by a Grant-in-Aid for Scientific Research (B) No. 06452317 followed by No. 08458120 from the Ministry of Education, Science, Sports and Culture of Japan.

- ¹A. M. Stoneham, *Theory of Defects in Solids* (Oxford, Clarendon, 1975), pp. 653–669.
- ²A. S. Nowick, in *Point Defects in Solids*, edited by J. H. Crawford and L. M. Slifkin (Plenum, New York, 1972), Chap. 3; E. Sonder and W. A. Sibley, *ibid.*, Chap. 4.
- ³W. Hayes and A. M. Stoneham, in *Crystals with the Fluorite Structure*, edited by W. Hayes (Oxford, Clarendon, 1974), Chaps. 2 and 4; A. B. Lidiard, *ibid.*, Chap. 3.
- ⁴J. H. Beaumont, W. Hayes, D. L. Kirk, and G. P. Summers, Proc. R. Soc. London, Ser. A **315**, 69 (1970).
- ⁵W. Hayes and J. W. Twidell, Proc. Phys. Soc. London **79**, 1295 (1962).
- ⁶Y. M. Aleksandrov, S. K. Batygov, K. V. Glagolev, V. N. Kolanov, V. N. Makhov, T. I. Syreishchikova, and M. N. Yakimenko, Fiz. Tverd. Tela (Leningrad), **24**, 1172, (1982) [Sov. Phys. Solid State **24**, 661 (1982)].
- ⁷N. N. Ershov, N. G. Zakharov, and P. A. Rodnyi, Opt. Spektrosk. **53**, 89 (1982) [Opt. Spectrosc. **53**, 51 (1982)].
- ⁸A. V. Agafonov and P. A. Rodnyi, Fiz. Tverd. Tela (Leningrad) **25**, 589 (1983) [Sov. Phys. Solid State **25**, 335 (1983)].
- ⁹A. V. Golovin, N. G. Zakharov, and P. A. Rodnyi, Opt. Spektrosk. **65**, 176 (1988) [Opt. Spectrosc. **65**, 102 (1988)].
- ¹⁰E. N. Melchakov, P. A. Rodnyi, and M. A. Terekhin, Opt. Spektrosk. **69**, 1069 (1990) [Opt. Spectrosc. **69**, 634 (1991)].
- ¹¹B. P. Sobolev, E. A. Krivandina, S. E. Derenzo, W. W. Moses, and A. C. West, in *Scintillator and Phosphor Materials*, edited by M. J. Weber, P. Lecoq, R. C. Ruchti, C. Woody, W. M. Yen, and R-Y. Zhu, MRS Symposia Proceedings No. 348 (Materials Research Society, Pittsburgh, 1994), p. 277.
- ¹²H. von Seggern and T. Voigt, J. Appl. Phys. **64**, 1405 (1988).
- ¹³Y. Iwabuchi, N. Mori, K. Takahashi, T. Matsuda, and S. Shionoya, Jpn. J. Appl. Phys., Part 1 **33**, 178 (1994).
- ¹⁴N. N. Ershov, N. N. Njkulin, and P. A. Rodnyi, Opt. Spektrosk. **44**, 411 (1978) [Opt. Spectrosc. **44**, 241 (1978)].
- ¹⁵N. N. Ershov, T. I. Nikitinskaya, V. M. Reiterov, and P. A. Rodnyi, Opt. Spektrosk. **45**, 1201 (1978) [Opt. Spectrosc. **45**, 935 (1978)].
- ¹⁶N. N. Ershov, Opt. Spektrosk. **46**, 612 (1979) [Opt. Spectrosc. **46**, 342 (1979)].
- ¹⁷N. N. Ershov, Zh. Prikl. Spektrosk. **44**, 427 (1986).
- ¹⁸K. Kawano, J. Tominaga, H. Satoh, R. Nakata, and M. Sumita, Jpn. J. Appl. Phys., Part 2 **29**, L319 (1990).
- ¹⁹R. Nakata, H. Satoh, J. Tominaga, K. Kawano, and M. Sumita, J. Phys. C **3**, 5903 (1991).
- ²⁰K. Kawano, H. Akahane, R. Nakata, and M. Sumita, J. Alloys Compd. **221**, 218 (1995).
- ²¹H. W. Verleur and A. S. Barker, Phys. Rev. **164**, 1169 (1967).
- ²²W. B. Lacina and P. S. Pershan, Phys. Rev. B **1**, 1765 (1970).
- ²³K. Kawano, R. Nakata, and M. Sumita, Jpn. J. Appl. Phys., Part 1 **32**, 1736 (1993).
- ²⁴K. Kawano, R. Nakata, and M. Sumita, Jpn. J. Appl. Phys., Part 1 **32**, Suppl. 32-3, 182 (1993).
- ²⁵S. Iida, K. Sakae, H. Terauchi, K. Kubota, T. Kojima, Y. Yamada, T. Kato, N. Nakamura, T. Kunimatsu, H. Yoshimoto, N. Ninomiya, and M. Den, Jpn. J. Appl. Phys., Part 1 **22**, 1444 (1983).
- ²⁶T. Ohya, Master's thesis, University of Electro-Comm., 1987.
- ²⁷K. Kawano, K. Katoh, and R. Nakata, J. Phys. Soc. Jpn. **66**, 1531 (1997).
- ²⁸B. Moine, B. Courtois, and C. Pedrini, J. Lumin. **45**, 248 (1990).
- ²⁹B. Moine, B. Courtois, and C. Pedrini, J. Lumin. **50**, 31 (1991).
- ³⁰K. Tanaka, Q. Zhuang, K. Tanaka, K. Kawano, and R. Nakata, J. Phys. Chem. Solids **57**, 307 (1996). In order to detect only trivalent Eu ions in alkaline earth fluorides, the ITC experiment is very effective for distinguishing them perfectly from divalent Eu ions because the formation of $\text{Eu}^{3+}\text{-F}^-$ electric dipoles can contribute to the displacement current generated by a thermal release of frozen dipoles. The Eu^{3+} fraction was estimated from the integral intensity of the ITC spectrum to be 3% of all the doped Eu ions with 0.1-mol% concentration.
- ³¹J. Röhler, in *Handbook on the Physics and Chemistry of Rare Earths*, edited by K. A. Gschneider, Jr., L. Eyring, and S. Hufner (North-Holland, Amsterdam, 1987), Chap. 71, pp. 453–545.
- ³²V. V. Ter-Mikirychev and T. Tsuboi, Prog. Quantum Electron. **20**, 219 (1996). Generally speaking, color centers are stabilized by doping appropriate impurities, in which color center lasers oscillate stably at room temperature. However, the capacity to endure radiation for a scintillator decreases in the presence of impurities.
- ³³C. P. Flynn, *Point Defects and Diffusion* (Clarendon, Oxford, 1972), Chaps. 3, 7, and 12.
- ³⁴B. D. Bartolo, *Optical Interactions in Solids* (Wiley, New York, 1968), Chap. 18.
- ³⁵A. Yariv, *Quantum Electronics*, 2nd ed. (Wiley, New York, 1975), pp. 184–193.